Journal of Catalysis 272 (2010) 309–314

Contents lists available at ScienceDirect

Journal of Catalysis

journal homepage: www.elsevier.com/locate/jcat

# Gas-phase coupling of reactive surfaces by oscillating reactant clouds

Daniel Bilbao, Jochen Lauterbach *

*Center for Catalytic Science and Technology, Department of Chemical Engineering, University of Delaware, Newark, DE 19716, USA*

ARTICLE INFO

*Article history:*
Received 16 October 2009
Revised 23 March 2010
Accepted 14 April 2010
Available online 14 May 2010

*Keywords:*
CO oxidation
Platinum
Oscillations

ABSTRACT

The collective, global behavior of a heterogeneous catalytic system depends on the effective communication of local reactivity variations to distant points in the system. One particularly efficient mode of communication occurs via partial pressure fluctuations in the gas-phase above the reactive surface. Although gas-phase communication has been implicated in a number of heterogeneous systems, the details of this coupling mechanism are lacking due to experimental difficulties in addressing local variations in surface and gas-phase activity simultaneously. Here, we take advantage of a spatially distributed system of isolated chemical oscillators to investigate the details of gas-phase communication in the $10^{-3}$ mbar range. Characterization of local gas-phase oscillations, in parallel with kinetic oscillations on the surface, provides a novel description of the surface/gas-phase interaction under reaction conditions. This analysis further allows for a quantitative estimate of the effective gas-phase coupling length scale observed in surface imaging experiments.



## 1. Introduction

Spatial coupling, which involves the communication of local reactivity to regions elsewhere in a system, underlies the fundamental behavior of many chemical systems over a wide range of operating conditions. Coupling in heterogeneous catalytic systems may occur through a combination of modes depending on the specific reaction conditions. At high gas-phase pressures (>1 mbar), coupling can be achieved when heat generated by an exothermic chemical reaction is transmitted through the catalyst itself to another location, perpetuating the surface reaction [1–3]. At lower pressures, heat released due to reaction may not be sufficient to transmit local reactivity variations through the catalyst and thermal coupling becomes less effective. Under such conditions, adsorbate diffusion on the catalyst surface provides relatively short range spatial coupling ($\sim 10^2$ μm), through the formation of traveling chemical waves. A third coupling mode, present in both high and low pressure situations, is gas-phase coupling, where local reaction rate variations are communicated via fluctuations in the partial pressure of reactants in the gas-phase above the surface. This relatively rapid, long-range coupling mechanism has been used to explain globally synchronized oscillations on single crystal surfaces under vacuum [4–6], coupling of individual grains on polycrystalline catalysts [7,8], and dynamic behavior on supported catalysts at elevated pressures [3,9,10]. A particularly impressive demonstration of the efficiency of gas-phase coupling was found in the development and synchronization of standing waves during CO oxidation on Pt(1 1 0) [11,12]. In general, the effects of gas-phase coupling in heterogeneous systems may be described as analogous to those of mixing in a CSTR system, in the sense that each action produces a uniform, spatially coupled system.

While these studies clearly established the presence of a gas-phase coupling pathway, the details of this mechanism have yet to be resolved. Generally, under high vacuum conditions, local reaction rate variations are assumed to affect the entire system instantaneously and uniformly [6,13,14]. In other words, the mean free path between molecular collisions is taken to be large enough that the system can be considered well-mixed, where any local kinetic activity is entrained by global reactor dynamics. While this description may be true far from the surface, this model fails near the surface which effectively behaves both as a sink and source of molecular species. In this work, we apply ellipsomicroscopy for surface imaging (EMSI) in parallel with scanning quadrupole mass spectrometry (SQMS) to investigate the gas-phase environment near the surface under dynamic reaction conditions. Utilizing CO oxidation on polycrystalline Pt as a model system, we show that the gas-phase near the surface is not uniformly mixed and that coupling between individual catalyst grains, by way of gas-phase communication, can be restricted by concentration gradients existing at the surface. Also, by defining the spatial limits of the concentration gradients above single catalyst grains with SQMS, we provide a quantitative estimate for the gas-phase coupling length scale in support of the qualitative, visual estimate provided by our EMSI data.

* Corresponding author.
*E-mail address:* lauterba@udel.edu (J. Lauterbach).

0021-9517/$ - see front matter © 2010 Elsevier Inc. All rights reserved.
doi:10.1016/j.jcat.2010.04.010

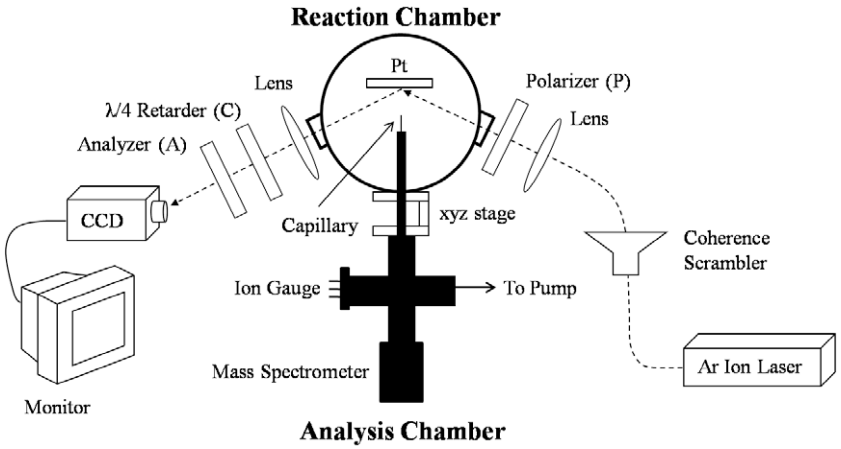


**Fig. 1.** Experimental setup consisting of a reaction chamber and an adjoining analysis chamber (black) used for scanning quadrupole mass spectrometer studies.

## 2. Experimental

A fundamental difficulty in addressing spatially localized activity is the selection of a model catalytic system which is able to provide meaningful results of broad relevance. Even more difficult, from a surface science perspective, is the problem of correlating local gas-phase variations above the surface to local kinetic activity on the surface. We address the former by using a polycrystalline foil catalyst, which can be considered representative of supported catalysts used industrially while still allowing for fundamental surface science studies [2,15]. In this way, the polycrystalline surface provides an experimental platform that is relevant across the spectrum of catalyst materials, from relatively basic single crystal surfaces to supported nanoparticle catalysts. The polycrystalline surface was prepared by annealing a Pt foil (Alfa Aesar, 99.997%) in $N_2$ to 1373 K for 12 h. Naturally, the polycrystalline surface contains a distribution of catalyst grains of varying crystallographic orientation and reactivity. Therefore, under particular reaction conditions, some grains existed in a stable, high-reactive, O-covered state, while other grains quickly poisoned to a CO-covered state. A smaller number of grains also exhibited self-sustained oscillations between the O and CO-covered states. Because kinetic activity on each grain was contained by the grain boundaries, with no observed diffusion coupling across these boundaries, the polycrystalline surface represented a spatially distributed system of isolated chemical oscillators, where gas-phase coupling was the only possible mode of communication between oscillators. These discrete oscillators were located on the surface using EMSI, an optical technique which allows for the detection of different adsorbates due to local differences in the optical properties of the surface [16]. A schematic of the entire experimental setup is shown in Fig. 1. The setup consisted of two adjoining vacuum chambers, denoted the reaction chamber and analysis chamber (black), which served as the SQMS, in Fig. 1. The reaction chamber contained the catalyst and reactant gasses and was surrounded by the equipment used for EMSI experiments. An Ar ion laser was used to generate the monochromatic light needed for EMSI, which was directed toward the surface by an optical fiber. The laser light was linearly polarized using a Glan–Thompson polarizer (P) before entering the reaction chamber. Upon reflection from the surface, the light became elliptically polarized and exited the reaction chamber toward a quarter-wave retarder (C), which returned the light to a linear polarization state which was then analyzed using a second polarizer (A). The final image is captured by a CCD camera and is recorded and stored on a DVR hard drive.

The key component of the SQMS setup consisted of a tapered glass capillary that was attached at the end of a probe which

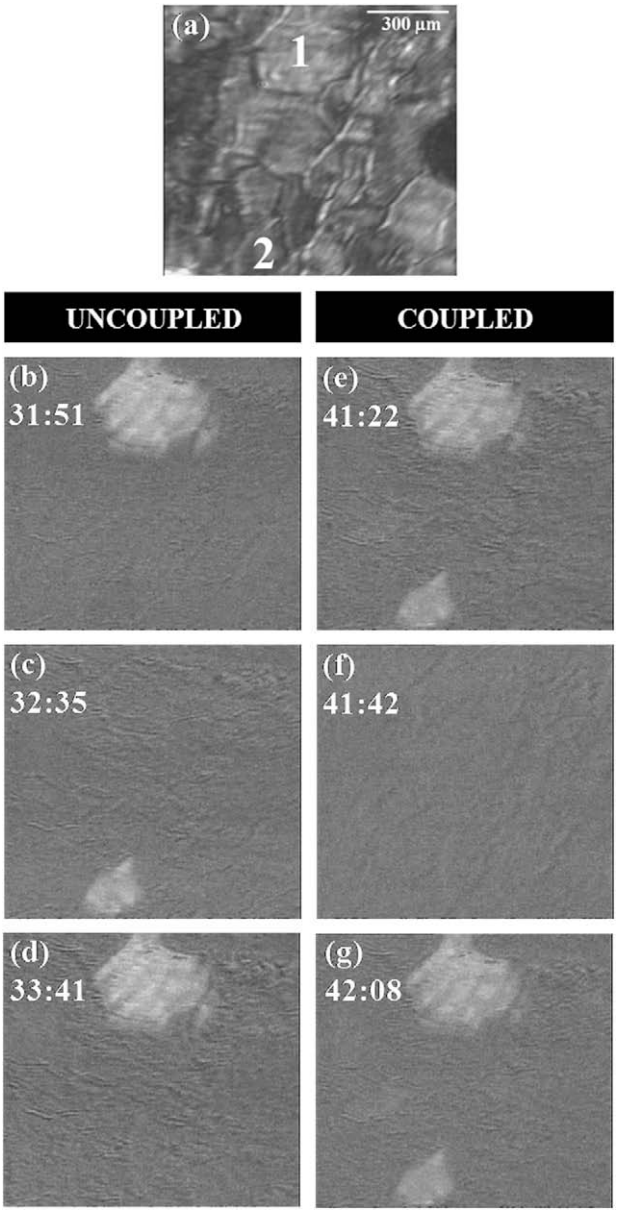


**Fig. 2.** EMSI snapshots of uncoupled (b–d) and coupled (e–g) oscillations on catalyst grains 1 and 2 (a). The grains appear light-gray when O-covered and dark-gray when CO covered ($p_{O_2} = 2.4 \times 10^{-3}$ mbar, $p_{CO} = 2.9 \times 10^{-4}$ mbar, and $T = 534$ K).

extended from the analysis chamber into the reaction chamber. A 50-μm orifice at the tip of the capillary enabled local sampling of the gas-phase environment in the reaction chamber at any point of interest around the reactive surface. The SQMS was attached to the reaction chamber through a *xyz* stage that allowed for the SQMS sampling probe to be positioned at various locations around the catalyst surface. In all experiments, an inert tracer species, Ar, was co-fed to the reactor along with reactants and was continuously monitored with the SQMS. Before quantification, all MS spectra were normalized to the Ar tracer concentration. This procedure allowed for experimental artifacts such as MS drift and mass transport restrictions caused by the proximity of the SQMS probe to the surface to be accounted for.

## 3. Results and discussion

Fig. 2a shows a raw EMSI image of the polycrystalline surface for reference. In this image, several grains, separated by dark grain boundaries, up to several hundred microns in size are visible. The grains labeled 1 and 2 in the image exhibited self-sustained oscillations under global reaction conditions of $p_{O_2} = 2.4 \times 10^{-3}$ mbar and $p_{CO} = 2.9 \times 10^{-4}$ mbar, at a surface temperature of 534 K. Fig. 1b–d show grains 1 and 2 oscillating, out of phase, between an O-covered (light-gray) and CO-covered (dark-gray) state with periods ranging from 90 to 180 s. This behavior is also illustrated graphically in Fig. 3, which plots the EMSI image intensity on grains 1 (upper curve) and 2 (lower curve) over the course of several oscillatory cycles on each grain at the beginning of the experiment. During the out of phase oscillations, the global $CO_2$ signal in the reaction chamber also remained relatively constant (see bottom panel of Fig. 5). This is due to the fact that the global $CO_2$ signal results from the superposition of the individual reaction rates for each of the oscillating grains. Therefore, while the grains continued to oscillate independently, local variations in the reaction rate on each grain were averaged out to generate a constant global signal.

After 40 min of out of phase oscillations, the oscillations on grains 1 and 2 became effectively coupled, as shown in Fig. 1e–f, oscillating in phase within one to two seconds of each other on a regular basis. The transition to the coupled state can clearly be seen by comparison with Figs. 3 and 4, which now shows multiple, synchronized oscillations on each of the two grains over a 700-s time period. Additionally, once coupling between grains 1 and 2, and presumably other oscillating grains outside of the EMSI image, was achieved, global gas-phase $CO_2$ oscillations with a period of 120 s were detected in the reactor (top panel of Fig. 5). It also worth noting that even during the time period where the system exhibited predominantly coupled behavior, there were still instances where individual grains exhibited activity independent of the global state. For example, one such occurrence can be seen at $t = 2600$ s in Fig. 4, where an oscillation cycle on grain 2 was observed approximately 50 s before the following cycle on grain 1. This type of behavior occurred somewhat infrequently, for example only one such discrepancy can be seen out of a total of nine oscillation cycles recorded in Fig. 4 but could possibly account for multi-peaked oscillations observed in the gas-phase, such as that at $t = 8150$ s in Fig. 5.

The fact that grains 1 and 2, separated by only 500 μm, repeatedly exhibited uncoupled behavior for extended periods of time is significant. This delay suggests that, while synchronization between the grains eventually developed over time, communication through the gas-phase was limited. This result was unexpected given the mean free path between molecular collisions, calculated from the kinetic theory of gasses, was on the order of 3 cm at these conditions. This theoretical estimate of the mean free path was longer than the dimension of the entire catalyst sample ($1 \times 1$ cm$^2$), and several orders of magnitude larger than the distance between grains 1 and 2. Therefore, under the typical assumption of a large mean free path relative to the system of interest, i.e., well-mixed conditions, coupling between these oscillators would be expected to be instantaneous, which was clearly not the case.

To better understand the apparent time delay for coupling, the SQMS was used to locally sample the gas-phase directly above grain 1 during the initial 40-min time period in which the grains remained uncoupled. In doing so, the contribution of local rate variations on the surface could be resolved in the gas-phase near the surface. Fig. 6 illustrates the local change in oscillation

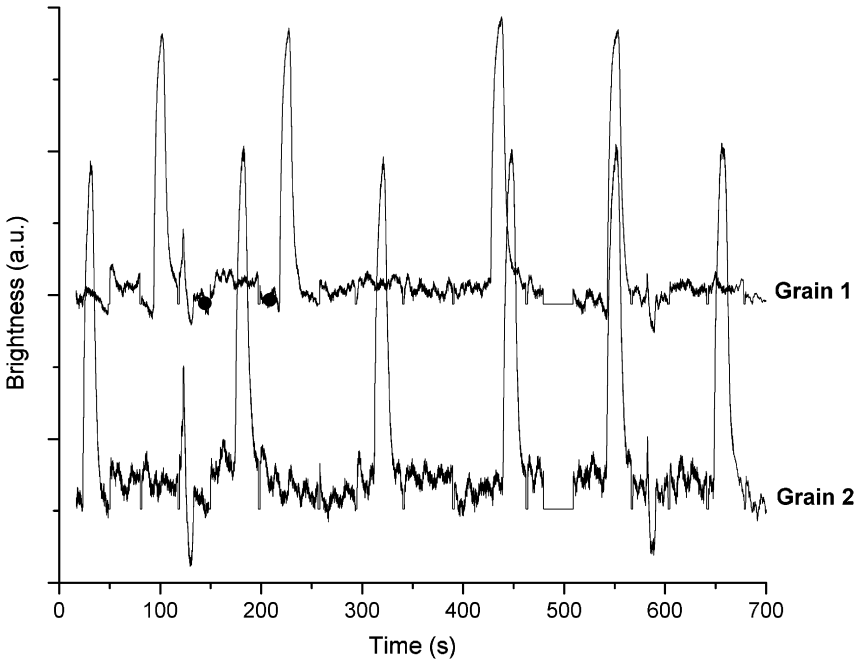


**Fig. 3.** Representative EMSI image intensity profile during uncoupled oscillations on grains 1 and 2.

amplitude for CO at various distances normal to the surface, along the $z$ axis (see Fig. 6 inset). The dataset in Fig. 6 terminates at an amplitude of 0.04 a.u., which represents a conservative estimate of the SQMS noise level. Most notably, the attenuation of the oscillatory CO signal in Fig. 6 implies that kinetic variations on the surface do not affect the entire gas-phase uniformly. Gas-phase regions within 800 μm of the surface are significantly affected by activity on the surface, while the gas-phase CO concentration beyond this point appears to be unaffected by the surface oscillations.

Additional insight into the attenuated oscillatory CO signal can also be gained by examining local gas-phase behavior near the surface under steady state, non-oscillatory conditions. Fig. 7 shows the local CO and Ar tracer concentration as a function of SQMS distance normal to the surface. Under steady state conditions, both the CO and Ar signals decreased as the SQMS approached the surface, although the change in CO concentration was more dramatic than that of Ar. This is due to the fact that CO adsorbs and subsequently reacts with O on the surface, in contrast to Ar that does not

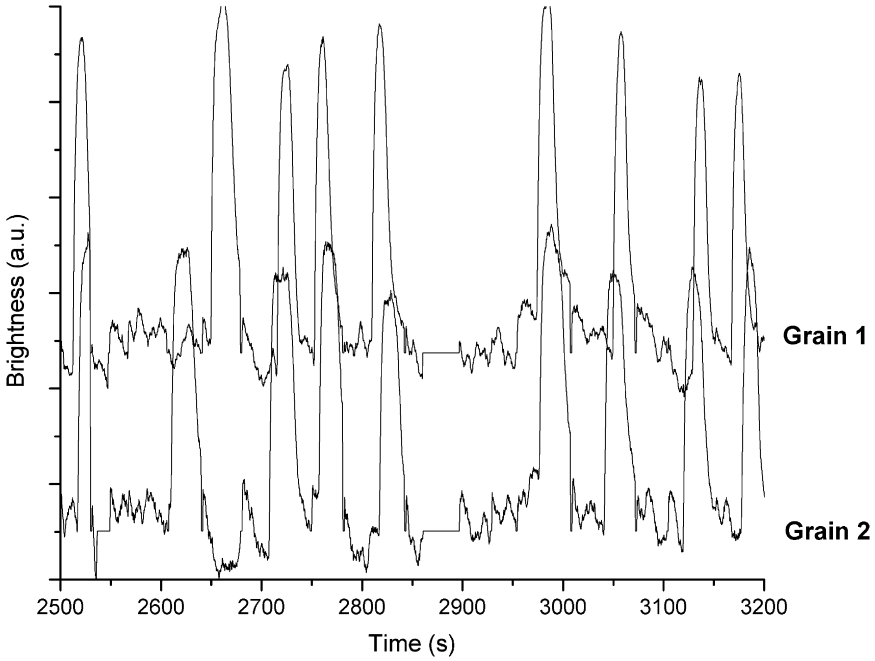


**Fig. 4.** Representative EMSI image intensity profile during uncoupled oscillations on grains 1 and 2.

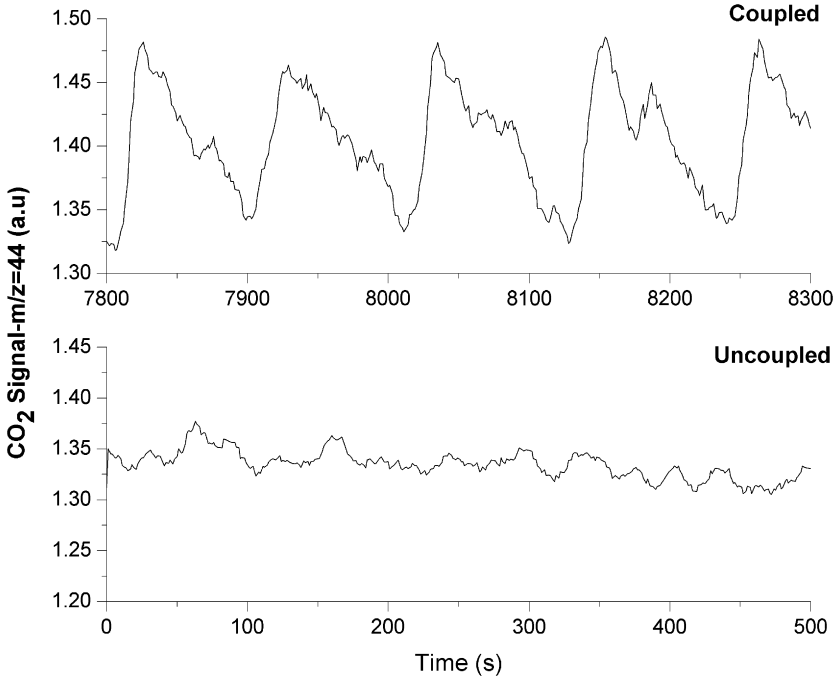


**Fig. 5.** Global $CO_2$ mass spectrometer signal during the uncoupled (bottom panel) and coupled (top panel) periods. Global scans were taken by locating the SQMS orifice 5 cm from the surface.

adsorb at these surface temperatures. Subsequently, the variation in the Ar signal represents only limitations associated with the transport of molecules into the confined space between the surface and the SQMS probe. Based on the Ar tracer data from Fig. 7, it is clear that the SQMS probe had no significant affect on reactant transport to the surface for the sampling locations of $z \geqslant 50$ μm used in the present work. Therefore, the CO concentration gradient detected within 200 μm from the surface under steady state reaction conditions is due entirely to surface-related processes (i.e., adsorption, reaction). This conclusion is further supported by the findings of Roos et al. [17], who reported similar concentration gradients normal to a Pt catalyst also during CO oxidation. The detected gradients may be the result of relatively frequent molecular collisions in the gas-phase, or possibly, the superposition of various directed flows of CO to the surface according to a $\cos(\theta)$ relation ($\theta$ being the angle between the surface normal and the specific angular adsorption channel). Irrespective of the source, the detection of concentration gradients identifies a system

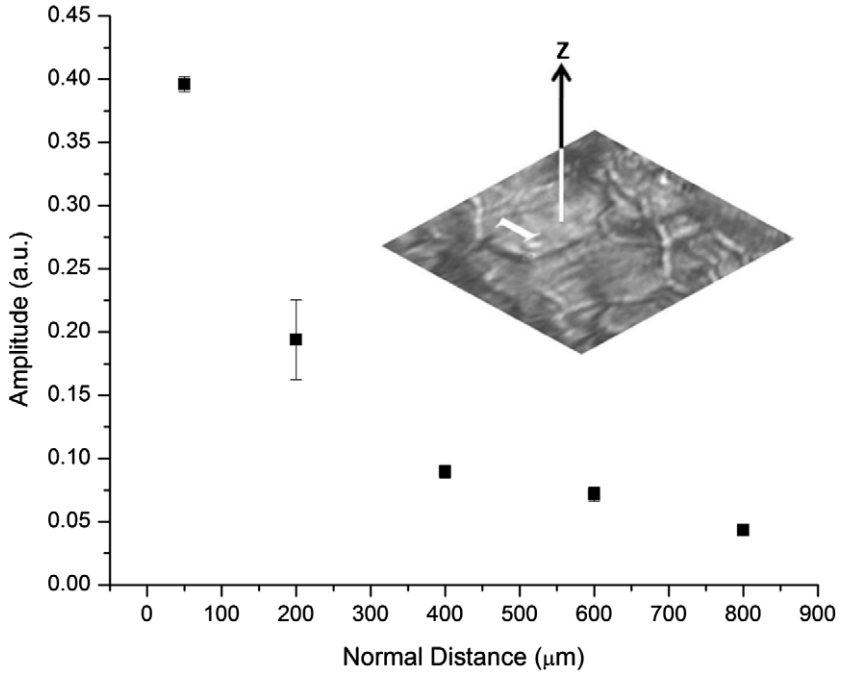


**Fig. 6.** Local CO oscillation amplitude due to kinetic oscillations on grain 1 at various distances from the surface.

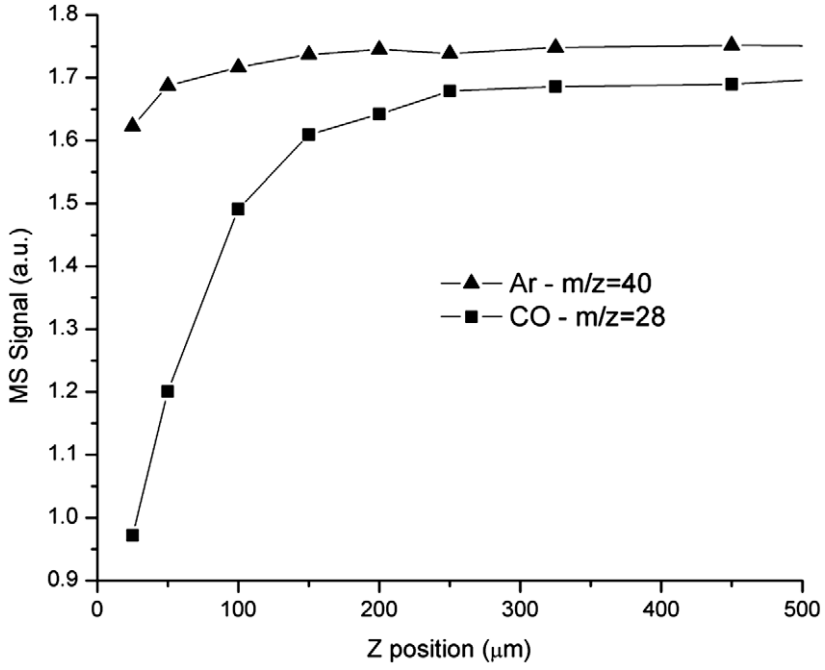


**Fig. 7.** CO and Ar concentrations for various SQMS probe distances normal to the reactive surface ($p_{O_2} = 1.3 \times 10^{-3}$ mbar, $p_{Ar} = 7.9 \times 10^{-5}$ mbar, and $T = 522$ K).

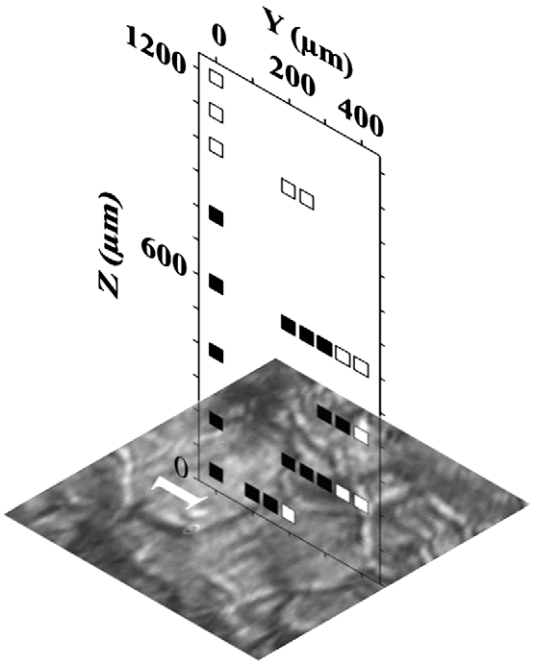


**Fig. 8.** Local gas-phase CO oscillations due to kinetic oscillations on grain 1. Filled data points mark locations where CO oscillations were detected with an amplitude $\geqslant$0.04 a.u. (MS noise limit), open data points denote locations where oscillations were not detected ($p_{O_2} = 2.4 \times 10^{-3}$ mbar, $p_{CO} = 2.9 \times 10^{-4}$ mbar, and $T = 534$ K).

that is not uniformly mixed to within a certain distance of the reactive surface. It follows that the established gradients could also account for the observed oscillatory signal attenuation (Fig. 6), and ultimately, the delayed synchronization of individual oscillating grains discussed previously.

The presence of concentration gradients normal to the catalyst surface further suggests that there is a finite length scale associated with gas-phase communication, where oscillators located within this particular distance are able to communicate effectively. To directly identify this length scale, it was necessary to define the spatial limits of local concentration oscillations in the gas-phase due to a single oscillating catalyst grain. To accomplish this, several points in the gas-phase above grain 1 were sampled with the SQMS, again surveying for local gas-phase oscillations due to oscillations on grain 1. Fig. 8 summarizes all sampling points, which fell on the *yz* plane oriented above grain 1 as shown. The filled data points indicate locations where gas-phase CO oscillations of amplitude $\geqslant$0.04 a.u. were detected, while the open data points denote locations where the oscillation amplitude fell below 0.04 a.u. and could not be quantified. The filled points therefore define the cross section of a cloud of oscillating CO concentration driven by oscillations on grain 1. This oscillating cloud expanded to 800 μm above the surface and up to 250 μm away from the lower boundary of grain 1 (located at $y = -100$ μm). The expanse of the cloud is of particular interest, as the span of the cloud can have a significant effect on the behavior of nearby oscillators. For example, the local supply of CO in the gas-phase may be depleted due to activity on a single grain up to 250 μm away from the CO supply, as shown in Fig. 8. This means that isolated grains, separated by up to twice this length, could be competing for the same finite, localized supply of CO. Therefore, kinetic information, such as an oscillation cycle, on a single grain may be communicated indirectly to distant grains 500 μm away by way of the shared CO supply. Obviously, the expanse of the oscillatory reactant cloud, and therefore the coupling dynamics, will depend on the relative size, reactivity, and proximity of the oscillating catalyst grains. However, even the small pressure variations (~4%) detected on the edges of the CO cloud above grain 1 have been shown to dramatically affect surface activity in global forcing experiments elsewhere [18,19] and would therefore be expected to play a significant role in the dynamics of this system.

## 4. Conclusions

In summary, we have used spatially isolated chemical oscillators in the form of catalyst grains on a polycrystalline Pt surface as a model system for the study of gas-phase coupling. By correlating local gas-phase variations to kinetic oscillations on individual grains, we were able to distinguish the gas-phase contribution of single catalyst grains from the global reactor background. With this capability, we demonstrated that the reaction environment near the surface is not uniformly mixed, as is typically assumed under vacuum reaction conditions, with concentration gradients extending several hundred microns into the gas-phase in a direction normal to the surface. By scanning the SQMS in 2-dimensions above a single oscillating grain, we were able to quantify regions in the gas-phase, or clouds, which were affected by the surface oscillations. The detection of oscillating reactant clouds above the dynamic surface ultimately provided a means of identifying an effective gas-phase coupling length scale, which for the conditions used in these studies ($p \sim 10^{-3}$ mbar), was found to be approximately 500 μm. This estimate is consistent with dynamic behavior observed during in situ surface imaging experiments, where coupling between individual catalyst grains separated by 500 μm was observed by means of synchronized kinetic oscillations.

## Acknowledgments

The authors acknowledge the US Department of Energy for support (or partial support) of this research (grant number DE-FG02-03ER15468), and Dr. C.M. Snively for assistance in designing the SQMS equipment.

## References

[1] E. Wicke, H.U. Onken, Chem. Eng. Sci. 43 (1988) 2289–2294.
[2] M.M. Slinko, A.A. Ukharskii, N.I. Jaeger, Phys. Chem. Chem. Phys. 3 (2001) 1015–1021.
[3] J.C. Kellow, E.E. Wolf, AIChE J. 37 (1991) 1844–1848.
[4] R. Imbihl, S. Ladas, G. Ertl, Surf. Sci. 215 (1989) L307–L315.
[5] M. Ehsasi, O. Frank, J.H. Block, K. Christmann, Chem. Phys. Lett. 165 (1990) 115–119.
[6] M. Eiswirth, P. Moller, K. Wetzl, R. Imbihl, G. Ertl, J. Chem. Phys. 90 (1989) 510–521.
[7] J. Lauterbach, H.H. Rotermund, Catal. Lett. 27 (1994) 27–32.
[8] N. McMillan, C. Snively, J. Lauterbach, Surf. Sci. 601 (2007) 772–780.
[9] S.Y. Yamamoto, C.M. Surko, M.B. Maple, J. Chem. Phys. 103 (1995) 8209–8215.
[10] M.A. Liauw, P.J. Plath, N.I. Jaeger, J. Chem. Phys. 104 (1996) 6375–6386.
[11] S. Jakubith, H.H. Rotermund, W. Engel, A. von Oertzen, G. Ertl, Phys. Rev. Lett. 65 (1990) 3013.
[12] A.v. Oertzen, H.H. Rotermund, A.S. Mikhailov, G. Ertl, J. Phys. Chem. B 104 (2000) 3155–3178.
[13] H. Levine, X. Zou, Phys. Rev. Lett. 69 (1992) 204.
[14] M. Falcke, H. Engel, J. Chem. Phys. 101 (1994) 6255–6263.
[15] L. Lietti, P. Forzatti, I. Nova, E. Tronconi, J. Catal. 204 (2001) 175–191.
[16] H.H. Rotermund, G. Haas, R.U. Franz, R.M. Tromp, G. Ertl, Science 270 (1995) 608–610.
[17] M. Roos, S. Kielbassa, C. Schirling, T. Haring, J. Bansmann, R.J. Behm, Rev. Sci. Inst. 78 (2007) 084104–084109.
[18] R.J. Schwankner, M. Eiswirth, P. Moller, K. Wetzl, G. Ertl, J. Chem. Phys. 87 (1987) 742–749.
[19] M. Eiswirth, G. Ertl, Phys. Rev. Lett. 60 (1988) 1526.